Power Routing Strategy for an Offshore-Onshore Bipolar VSC-HVDC Interconnector

Marchand, J.; Perilla , A; Garapati, M. ; Gonzalez-Longatt, Francisco; Rueda Torres, J.L.

Citation (APA)
Marchand, J., Perilla , A., Garapati, M., Gonzalez-Longatt, F., & Rueda Torres, J. L. (2023). Power Routing Strategy for an Offshore-Onshore Bipolar VSC-HVDC Interconnector. In *Proceedings of the 2023 IEEE Belgrade PowerTech* (pp. 1-6). (2023 IEEE Belgrade PowerTech, PowerTech 2023). IEEE. https://doi.org/10.1109/PowerTech55446.2023.10202854

Important note
To cite this publication, please use the final published version (if applicable).
Please check the document version above.

Power routing strategy for an offshore-onshore bipolar VSC-HVDC interconnector

J. Marchand, A. Perilla, M. Garapati
Dept. of Electrical Power Engineering
Delft University of Technology
Delft, Netherlands
M.Garapati@student.tudelft.nl

F. Gonzalez-Longatt
Department of Electrical Engineering
University of Exeter
Exeter, England
F.M.Gonzalez-Longatt@exeter.ac.uk

J.L. Rueda Torres
Department of Electrical Engineering
Delft University of Technology
Delft, Netherlands
J.L.RuedaTorres@tudelft.nl

Abstract—**Distantly-located offshore energy hubs need to be connected to the shore via High Voltage Direct Current (HVDC) links to allow for an efficient bulk power exchange. A bipolar configuration of the HVDC link is suitable for a point-to-point connection, as it provides redundancy, and, therefore, a larger reliability, e.g. half of the rated transfer capacity can still be transferred via one of the poles in case of a fault occurring on the other pole. Nevertheless, a control strategy of the converters that can effectively enable a situation-dependent power routing between the two poles constitutes a research challenge. In this paper, two control strategies are proposed for the offshore Modular Multi-level Converters (MMCs) of a bipolar HVDC link connecting a 2 GW offshore hub to the shore. The strategies, based on DC current and DC voltage measurements, respectively, enable to track and adjust the amount of power flowing through each pole of the link. Real-time digital simulations show that both strategies can effectively route the power exchanges through the bipolar HVDC link, e.g. operation under balanced or unbalanced conditions. The strategy based on DC current seems more suitable to manage the dynamic performance of the HVDC link.**

Index Terms—**Electromagnetic Transient (EMT) simulation, High Voltage Direct Current (HVDC) links, large-scale offshore networks, DC power management.**

I. Introduction

To fulfill the Paris Agreement [1], multi-GW offshore energy systems (e.g. wind-hydrogen hubs) should be urgently developed, e.g. the North Sea Wind Power Hub (NSWPH) consortium considers capacities around 65 GW and 20 GW of offshore wind and electrolysis for 2030, respectively [2].

High Voltage Direct Current (HVDC) links using Voltage Source Converter (VSC) have become the preferred technology for point-to-point electrical power transmission between offshore and onshore energy systems. VSC-HVDC links can effectively help to manage long-distance power transfers and also provide ancillary services (e.g. primary voltage control, black-start) [3].

Unlike the Line Commutated Converter (LCC) technology, VSCs are also able to operate when connected to weak AC systems [3]. Nevertheless, the cost-effective deployment of diverse VSC technologies in multi-GW scale (e.g. capacities above 2 GW and voltages above ±500kV) is hindered by the lack of operational experience and standardisation [4].

The topology of VSC-HVDC links should also be carefully studied. In 2 GW point-to-point interconnections, links with a bipolar topology (in which two Modular Multilevel Converters (MMCs) are connected at each side of the HVDC link), are an attractive option: First, in case of a converter outage or a line outage, half of the total capacity can still be transmitted by switching to a monopolar type of operation [5]. Second, if equipped with an appropriate control strategy, this topology can allow for more operational margin to safeguard a certain transfer capacity (e.g. in case of unavailability of one pole, it is still possible to transfer half of the total rated capacity by using the other pole) [3], [5].

Real-world examples of VSC bipolar links remain scarce: BritNet between the United Kingdom and the Netherlands (two LCC monopoles); SAPEI between Sardinia and Italy (LCC bipole); INELFE between France and Spain (two VSC monopolar links) [3]. However, it should be noted that the above-mentioned links are interconnectors operating between two strong synchronous systems.

Besides, there is a lack of solutions for adaptive power management performance in such interconnectors (especially for the bipolar configuration) when they are connected to a weak system, such as an offshore wind-hydrogen hub. Furthermore, in [6], one of the first power flow control strategies for VSC-HVDC bipolar links is presented. This and other recently published strategies are confined by the assumed symmetric operation of the the two poles of bipolar VSC-HVDC links (i.e. no applicability in case of considering a failure of one of the poles).

The aforesaid research gaps are of concern in this paper. For sake of illustration and feasibility, the rigid bipolar topology, in which both the offshore and onshore converter stations are grounded, has been chosen. The key technical contribution of this paper is to propose a control method to effectively manage the power sharing among the two poles of the offshore converter stations of a bipolar VSC-HVDC transmission link. The method can be deployed based on the needs of the operator, e.g. power routing during normal and exceptional operation conditions. The subsequent sections are organised as follows. In Section II, the hub's model layout is outlined. In Section III, the control strategy and its implementation in real-time digital simulation are presented. Real-time digital simulations are discussed in Section IV. Concluding remarks are summarized in Section V.

II. Modelling Aspects

The RSCAD® FX software package of the Real-Time Digital Simulator (RTDS) developed by RTDS Technologies Inc. has been chosen to perform the electromagnetic transient (EMT) modelling and simulations presented in this paper. This section focuses on essential modelling aspects of the hub.

A. Baseline model of the hub

The baseline model and its parameters are detailed in [7]. The hub consists of four offshore wind power plants (each one feeding a rated power of 500 MW to the hub) and two offshore MMC stations (each one rated at 1 GW).

- Each wind power plant is connected to the common bus of the hub via a back-to-back converter, a transformer, and a 66 kV HVAC cable. The plant also includes Permanent Magnet Synchronous Generators.
- Each MMC belongs to a monopolar link, which is connected to an ideal voltage source representing a strong DC network. One of the MMCs is grid-forming, whereas the other one is grid following. The voltage of the HVDC links is ± 640 kV.

This baseline model has been modified to turn the two HVDC links into a single bipolar link as shown in Fig. 1. The 1 GW onshore and offshore MMC stations have similar parameters. The onshore station is connected to an ideal AC source, which represents the connection to a strong onshore power system.
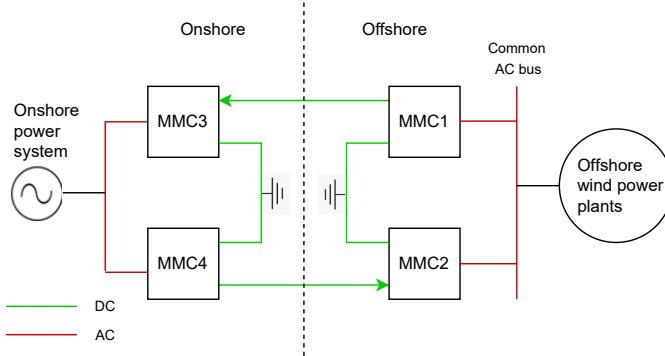

Fig. 1.   Topology of the offshore-onshore bipolar HVDC transmission link.

B. Control of the MMC stations

MMC3 (onshore positive pole) and MMC4 (onshore negative pole) as well as MMC1 (offshore positive pole) and MMC2 (offshore negative pole) are represented by the average library model MMC5 of RSCAD® FX, which is schematically illustrated in Fig. 2. Their settings are given in [7]. The two added onshore converters control the DC voltage at each pole of the link.

1) MMC1: One of the offshore MMCs should set the reference voltage and frequency in the weak offshore network. This is done by the grid forming MMC-1, which operates in V/F control mode. A PI controller takes as input the difference between the reference and measured voltage at the common bus. The output of the PI controller is the direct voltage

reference of MMC1, which is then converted to the ABC frame to generate the modulation waveforms of the converter. The control scheme is detailed in [7].

2) MMC2: Because the grid following MMC2 operates in parallel with the V/F controller of MMC1, the outer control loop of MMC2 should to be modified as described in Section III, as only one converter shall control the voltage of the common bus.
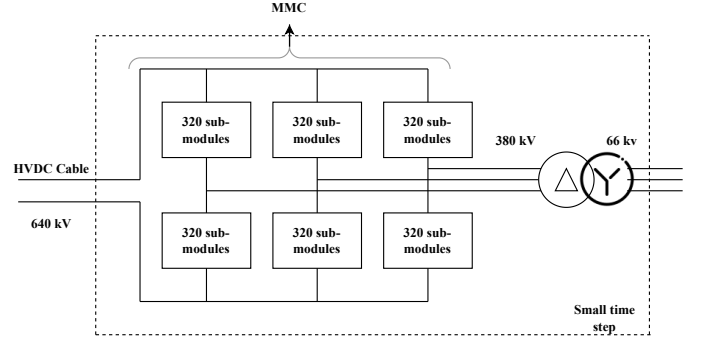

Fig. 2.   Assumed MMC representation

III. Modified Outer Current Loops of MMC2

A. Decoupling of active and reactive currents (I_d, I_q)

MMC1 sets the reference angle of the voltage. Based on this reference, the grid side converters of the wind generators, which are grid following (when operating in non-islanded mode), modify the local voltage angle at their terminal in order to control the power flowing through the HVAC cables. MMC2 is grid following. It is responsible for determining the share of active power flowing through each converter. The proposed control strategy for power sharing bases on the decoupling of active and reactive current. Basically, the total complex power S flowing through one of the MMCs can be written as the product of the complex voltage and complex conjugated current:

$$V = V_d + jV_q \tag{1}$$

$$I = I_d + jI_q \tag{2}$$

$$S = P + jQ = VI^* = (V_dI_d + V_qI_q) + j(V_qI_d - V_dI_q) \tag{3}$$

Considering Vq=0, as it is done in the Phase Lock Loop (PLL), the equation of S is simplified to

$$S = P + jQ = V_dI_d - jV_dI_q \tag{4}$$

from which the expression of the active power can be derived

$$P = V_dI_d \tag{5}$$

Note in (5) that the active power flowing through MMC2 P is proportional to the active current I_d flowing through this MMC. It is therefore possible to control P by changing the active current reference of MMC2. In order to set this active current reference, an outer loop is created in the controller of

MMC2. The outer loop takes a user defined active power set-point as input, as well as current and voltage measurements. The outputs of the outer loop are the reference active and reactive currents (the reactive current reference can be set to zero). These references are then passed on to the inner loop, which outputs the modulation waveforms used to control the submodules of the MMC. It should be noted that in the baseline model, the outer loop was simplified as indicated by (6) and (7), cf. [7].

$$i_{d,ref} = I_{ref}^d \tag{6}$$

$$i_{q,ref} = 0 \tag{7}$$

where $i_{d,ref}$ is provided by the user via a slider in the Run-time simulation environment of RSCAD® FX. This simplified mode of operation is kept as such during the initialisation phase of the simulation. A dial is used in Runtime to switch from the simplified outer current loops described in [7] to the modified loops proposed in this paper.

The higher $I_{d,ref}$, the more active power flows through MMC2. The remaining power flows through MMC1 based on the following equation of nodal power balance:

$$P_{MMC1} = \sum_{n=1}^{4} P_{GSCn} - P_{MMC2} \tag{8}$$

Two power sharing strategies are presented in the following sub-sections, and their feasibility is ascertained in Section IV.

B. Control Strategy Based on DC Current

A first control strategy is based on DC current control. The signals used to generate the reference for the inner loop $i_{d,ref}$ are current signals measured on the DC side. The underlying principle is that in balanced operation (i.e. when the same amount of power flows through each converter) the ground current i_{ground} must be equal to zero. In that way, both poles will be operated in a symmetrical manner regarding current, power and voltage. The zero ground current condition is expressed by

$$i_{ground} = i_{DCn,1} - i_{DCp,2} = 0 \tag{9}$$

which translates into the following condition on MMC2 output current:

$$\left(\frac{i_{DCn,1} + i_{DCp,2}}{2} \right) - i_{DCp,2} = 0 \tag{10}$$

Therefore, in balanced conditions, the goal of the PI controller in the new control strategy is to nullify the ground current, based on (9). In order to vary the share of power flowing through each MMC, a coefficient k_{sh} is introduced in (11).

$$\left(\frac{i_{DCn,1} + i_{DCp,2}}{k_{sh}} \right) - i_{DCp,2} = 0 \tag{11}$$

with $k_{sh} = 2$ in balanced conditions.

C. Control Strategy Based on DC Voltage

The power sharing control strategy presented in this section is inspired from the DC voltage droop control, which is the common control strategy used in Multi-terminal DC (MTDC) systems for power balancing between the multiple converters [8], [9].

The principle of DC voltage droop control is to measure the active power deviation (from a power reference) and to adapt the value of the DC voltage to oppose this deviation. The magnitude of the reaction to a power deviation is deter- mined by the droop coefficient k_{droop}, which is negative and selected by the user. In case of a power deviation event, the deviation will be absorbed by all the converters belonging to the system in order to remain in a balanced situation. The droop control prevents, for instance, that only one of the converters absorbs all the power deviation. The droop method is based on the proportional relation which can be written between the voltage difference between both ends of a line, and the power flowing through this line [9]:

$$V_{DC,\,ref} = V_0 + k_{droop} * (P_{meas} - P_0) \tag{12}$$

where the subscript 0 indicates the reference value achieved by power flow calculation for a pre-disturbance steady-state condition [8].

In the DC voltage control implemented in this paper, however, the goal is not to adapt the DC voltage as response to a power deviation (as for droop control), but to modify the DC voltage in order to achieve a different distribution of the active power between the two offshore converters. In order to do so, the power deviation between an active power reference determined by the user and an initial (arbitrary) reference is calculated, and multiplied by a positive coefficient k_{P-V} in order to produce a DC voltage reference, according to

$$V_{DC,\,ref} = V_0 + k_{P-V} * (P_{ref} - P_0) \tag{13}$$

where the initial reference point (V_0, P_0) = (640 kV, 0 MW) has been (arbitrarily) chosen to be the origin of the P-V slope, which can be determined as illustrated in Fig. 3. The power reference is the product of the measured AC active power at the common bus of the hub and a coefficient between 0 and 1 which can be varied by the user thanks to a slider available in the Runtime environment of RSCAD® FX. The P_{AC}-$V_{DC,MMC2}$ curve indicated in Fig. 3 can be fitted by a linear function, with the coefficient k_{P-V} being the slope of this function.

It is important to note that the goal of this control strategy differs from the classical droop control, in which a coefficient is chosen so that the converter adapts its voltage according to the incoming power. Here, a coefficient is determined so that the converters share power corresponding with a given voltage reference.

IV. RTDS BASED FEASIBILITY TESTS

In this section, the performance of the I_{DC} and V_{DC} control strategies in terms of stability and response time are ascertained under two severe scenarios:
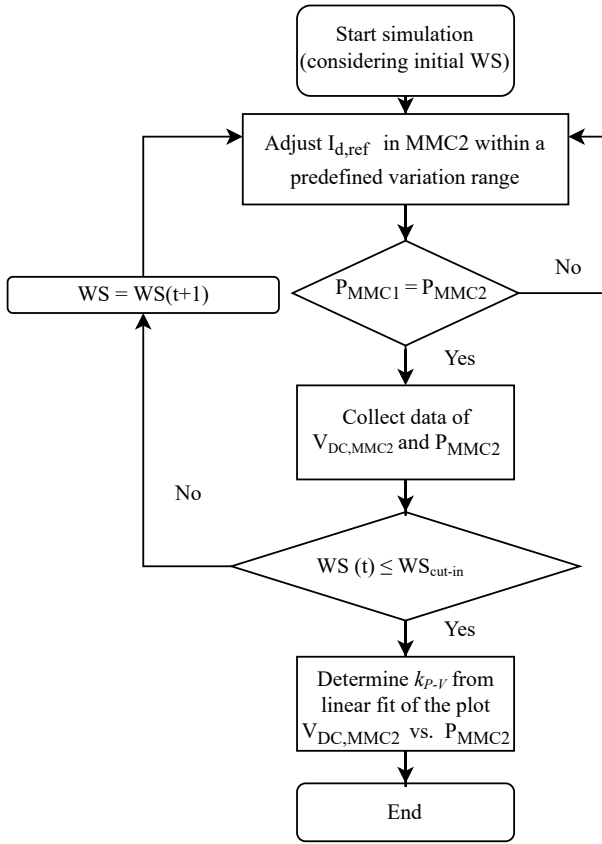
3

Fig. 3. Flowchart of the generation process for the P-V graph used in the V_{DC} control method (WS: wind speed).

- Scenario 1: a sudden wind speed change (case of the power sharing in balanced conditions).
- Scenario 2: unloading and reloading of MMC1 (extreme case of power sharing variation control order).

A. Scenario 1: Wind Speed Change

In this scenario, the wind speed is varied from 10 to 15 m/s as depicted in Fig. 4(a), whereas the power sharing between the two MMCs shall be maintained in balanced conditions.

Different measurements done in RSCAD® FX during this scenario are shown in Fig. 4. It can be seen that the I_{DC} and V_{DC} based control strategies can effectively stabilize and lead to comparable magnitudes of DC current and voltage, cf. Figs. 4(c)-(d). The active power in each MMC also increases, but a small overshot can be seen in Figs. 4(g)-(h). This overshoot is caused by the sudden wind speed increase, which creates a saturation in the pitch controller of the wind generators. The saturation stems from the rate limiter present in the pitch controller, representing the mechanical limitation of the pitch limiter.

Furthermore, it can be noticed that the power sharing is least altered in balanced conditions when using the I_{DC} control strategy, i.e. the time variation of ground current in Fig.4(d) shows an appreciable deviation when the V_{DC} control strategy is applied.

Furthermore, the AC voltage at the common bus increases from 0.8 to 0.95 pu, cf. Fig. 4(f). Ideally, this voltage should remain constant at 1 pu. The fact that a low AC voltage is observed at low wind speed is independent from the proposed control strategies (i.e. the same drop was observed when the outer loop of MMC2 for reactive power support was disabled). In fact, the reactive power reference was kept fixed at zero in this scenario. Alternatively, MMC2 can be configured to provide reactive power support to the common bus in case of voltage drop.

B. Scenario 2: Unloading and Reloading of MMC1

Being able to control the power sharing between MMC1 and MMC2 can be very useful, for instance, when doing maintenance on one pole. The application of the proposed control strategies for such purpose is illustrated as follows:

1) Unloading of MMC1: In this condition, the wind speed is maintained constant at 10.5 m/s. This value has been chosen because it equals half of the rated system capacity. Hence, the power can be shared as wanted between the two MMCs. Here, the power is initially equally shared between MMC1 and MMC2. At 0.5 s, the system is ordered to transfer the total power through MMC2, therefore unloading MMC1. The time responses are shown in Fig. 5: on the left column, the power sharing set-point has been given in the Runtime environment of RSCAD® FX as a step function, cf. left Fig 5(a), in order to represent an extreme operational change. On the right column, the set-point has been given as a ramp function, cf. right Fig 5(a), to ascertain if a less extreme operational change would entail an improved performance. The results for I_{DC} control are presented in blue, whereas those for V_{DC} control are presented in red. Three main observations can be made from these graphs:

- MMC1 cannot be completely unloaded and remains energised, cf. Fig. 5(d).
- A voltage drop (both AC and DC) unavoidably occurs when a step-wise set-point adjustment is done, cf. left Fig 5(b) and left Fig 5(e). Whereas this drop can be avoided by a ramp-wise set-point adjustment, cf. right Fig 5(b) and right Fig 5(e).
- Although the two control strategies seem to perform very well and can lead to comparable performances, the I_{DC} control is slightly faster than the V_{DC} control, cf. Figs. 5(f). A broader performance comparison, including optimal tuning of the two strategies will be addressed in a future subsequent research work.

2) Re-loading of MMC1: After unloading MMC1, the reverse operation is applied, to bring the system back to an equal power sharing between the two MMCs. The time responses are shown in Fig. 6. In this condition, a clear difference between the two control strategies can be seen: the V_{DC} baaed control (cf. time responses plotted with red lines) leads to large oscillations at a frequency of 5.6 Hz, whereas stable signals occur when using the I_{DC} based control (cf. time responses plotted with blue lines). Even if the same steady-state is reached after about 10 seconds, the signals are already
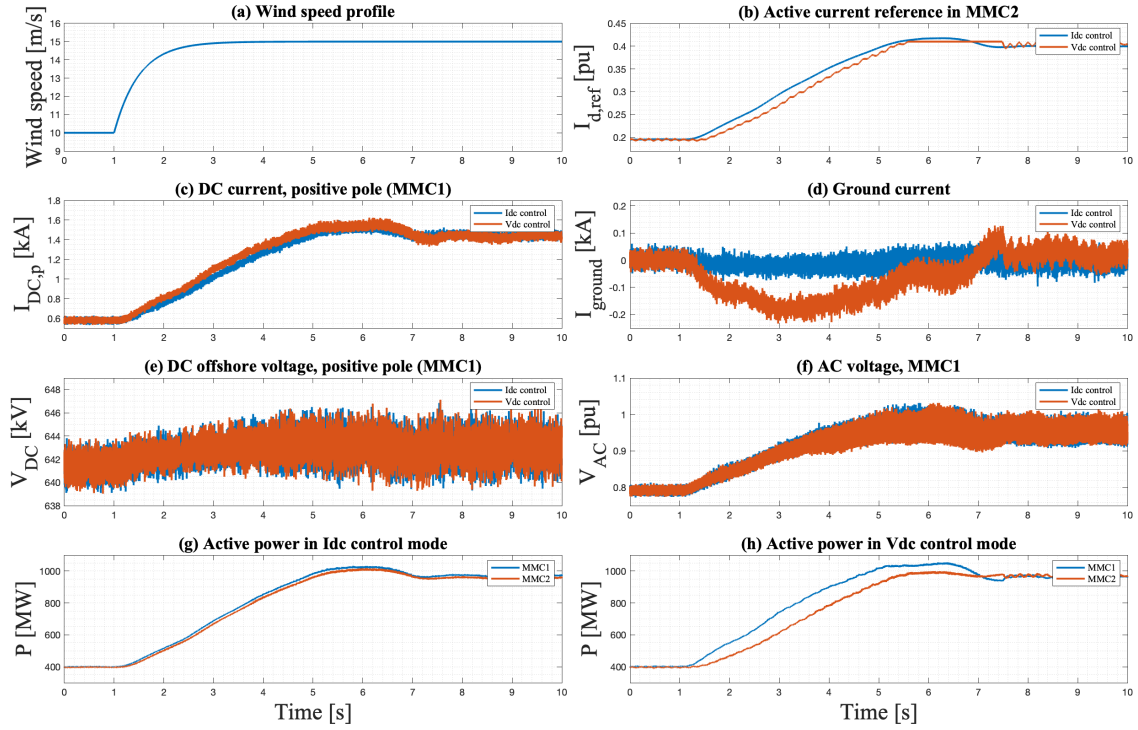
4

Fig. 4. MMCs' time responses when deploying the proposed I_{DC} and V_{DC} control strategies under a wind speed change from 10 m/s to 15 m/s.
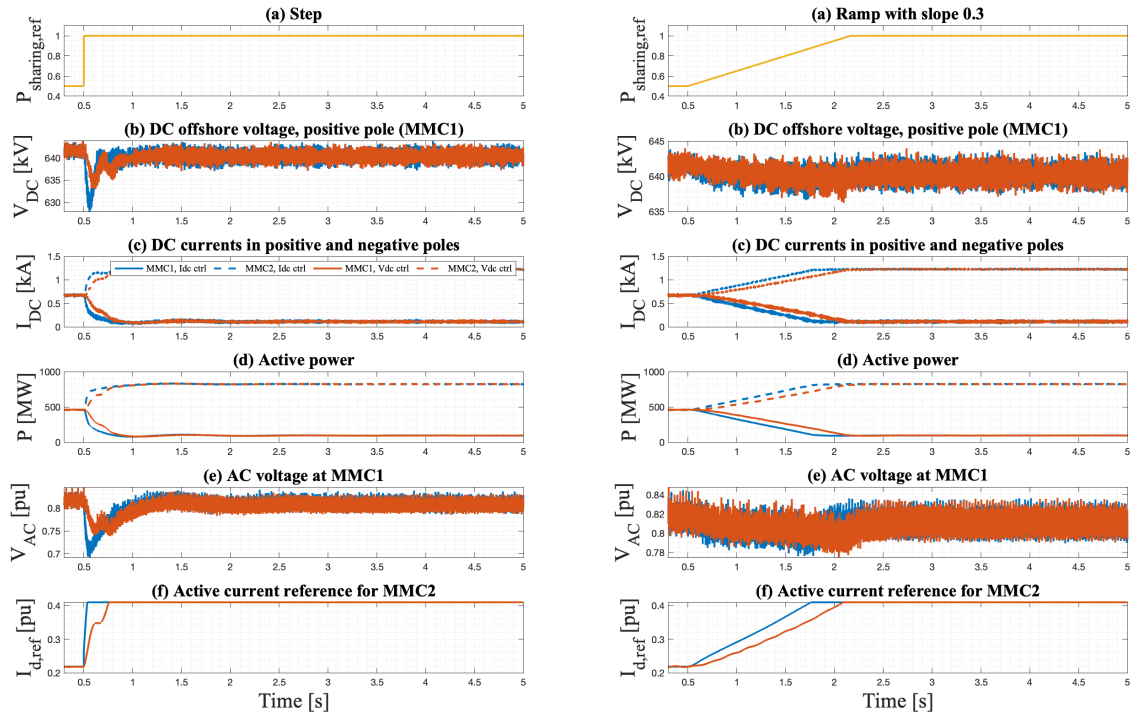

Fig. 5. MMCs' responses due to I_{DC} and V_{DC} control at MMC2 to tackle the unloading of MMC1 at a constant wind speed of 10.5 m/s.
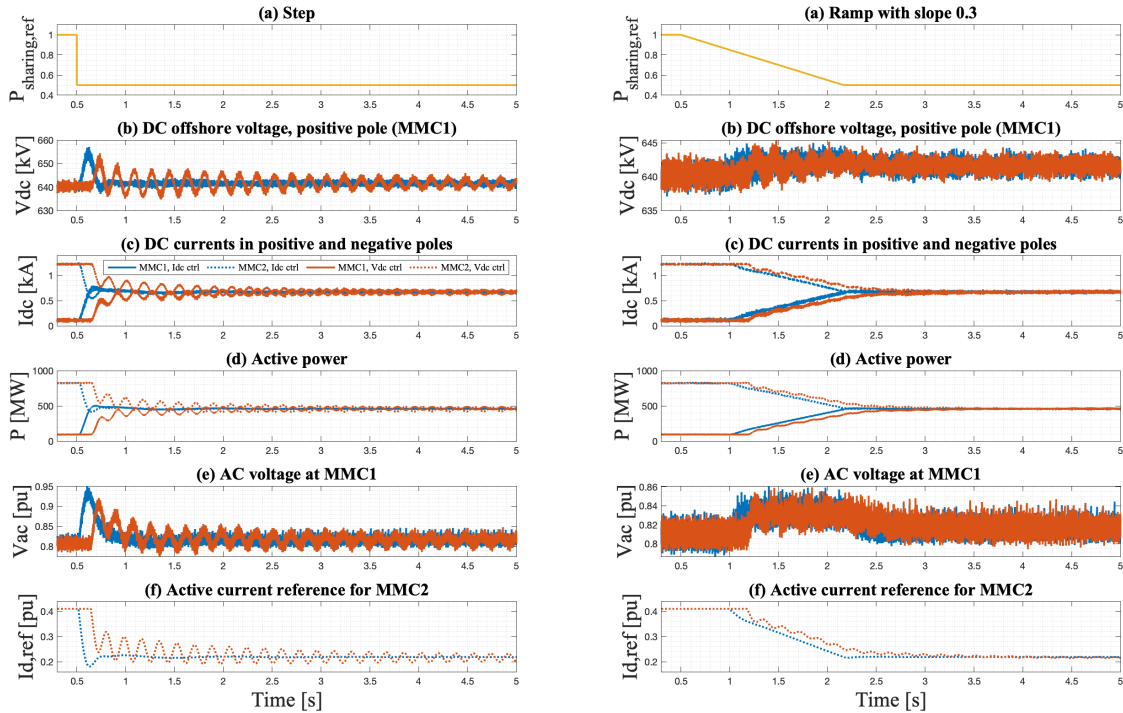
Fig. 6. MMMCs' responses due to I_{DC} and V_{DC} control at MMC2 to tackle the re-loading of MMC1 at a constant wind speed of 10.5 m/s.

settled in less that 1 second in the case of a step-wise set-point adjustment by using the I_{DC} based control. The latter is relevant for safeguarding the dynamic voltage response of the HVDC link.

V. CONCLUSIONS

This paper focuses on the the challenge of developing a power routing strategy for GW scale offshore energy hubs. Real-time EMT simulations are done to properly capture the fast dynamics of such zero inertia system. The EMT model of a 2 GW offshore wind energy hub presented in [7] is taken as a starting point, and upgraded to include a bipolar HVDC transmission link and two onshore MMCs. Two control strategies are proposed to effectively manage the power sharing among the two poles of the offshore converter stations of a bipolar VSC-HVDC transmission link. The strategies, based on DC current and DC voltage measurements, respectively, modulate the outer active power control loop of one of the offshore MMCs. The performed simulations show that both strategies can lead to comparable performance when deployed for balanced power sharing under sudden wind speed changes. The control strategy based on DC current seems faster and more effective to prevent undesirable oscillations that can jeopardize the dynamic performance of the HVDC link. Further research will be carried out (e.g. response under DC faults, optimal control) to deeply investigate the robustness of both power sharing strategies.

VI. ACKNOWLEDGEMENT

The authors thank the experts and technical support staff of RTDS Technologies Inc. for the insightful discussions during the execution of this research.

REFERENCES

[1] United Nations. Paris Agreement. https://unfccc.int/sites/default/files/english_paris_agreement.pdf, 2015. Accessed: 2021-08-03.

[2] North Sea Wind Power Hub. Six concept papers, one storyline. https://northseawindpowerhub.eu/vision/, 2019. Accessed: 2020-12-23.

[3] ENTSO-E. HVDC Links in System Operations. Technical report, ENTSO- E, Avenue de Cortenbergh 100, 1000 Brussels, Belgium, 2019.

[4] G. Donnini G. Giannuzzi M. Renieri R. Zaottini C. Pisani B. Aluisio A.Urbanelli Ch.Vergine L. Michi, E.M. Carlini. System dynamic behaviour challenges: operating experience and future trends. 2019 AEIT HVDC International Conference (AEIT HVDC), 2019.

[5] Siemens AG. High Voltage Direct Current Transmission – Proven Technol- ogy for Power Exchange. Technical Report E50001-U131-A92-V2-7600, Siemens AG, Power Transmission and Disttribution High Voltage Division Pstfach 3220 91050 Erlangen Germany, 2011.

[6] Y. Liu B. Li W. Wen B. Li, W. Wang. Research on power flow calculation method of true bipolar vsc-hvdc grids with different operation modes and control strategies. International Journal of Electrical Power Energy Systems, 2021.

[7] S. Ganesh, A. Perilla, J. Rueda Torres, P. Palensky, A. Lekić, and M. van der Meijden. Generic emt model for real-time simulation of large disturbances in 2 gw offshore hvac-hvdc renewable energy hubs. Energies, 2021.

[8] CIGRE - Working group B4.57. Guide for the Development of Models for HVDC Converters in a HVDC Grid. Technical report, CIGRE, 2014.

[9] [9] R. Irnawan. Planning and control of expandable multi-terminal VSC-HVDC transmission systems. PhD thesis, Aalborg University Denmark, 2018.